

Lysozyme Net Charge and Ion Binding in Concentrated Aqueous Electrolyte Solutions

Daniel E. Kuehner,^{†,‡} Jan Engmann,^{†,§} Florian Fergg,^{†,||} Meredith Wernick,[†]
Harvey W. Blanch,[†] and John M. Prausnitz^{*,†,⊥}

Department of Chemical Engineering, University of California, Berkeley, California 94720, and
Chemical Sciences Division, Lawrence Berkeley National Laboratory, Berkeley, California 94720

Received: September 24, 1998

Hydrogen-ion titrations were conducted for hen-egg-white lysozyme in solutions of potassium chloride over the range pH 2.5–11.5 and for ionic strengths to 2.0 M. The dependence of lysozyme's net proton charge, z_p , on pH and ionic strength in potassium chloride solution is measured. From the ionic-strength dependence of z_p , interactions of lysozyme with potassium and chloride ions are calculated using the molecular-thermodynamic theory of Fraaije and Lyklema.¹ Lysozyme interacts preferentially with up to 12 chloride ions at pH 2.5. The observed dependence of ion–protein interactions on pH and ionic strength is explained in terms of electric-double-layer theory. New experimental pK_a data are reported for 11 amino acids in potassium chloride solutions of ionic strength to 3.0 M.

1. Introduction

Salt ions play an important role in protein–protein interactions in aqueous solutions at all ionic strengths. At low salt concentrations, ions stabilize proteins in solution via reduction of electrostatic repulsion between charged protein macromolecules (i.e., the salting-in effect). As the salt concentration increases, repulsive electrostatic interactions are further screened; other protein–protein forces (notably attractive Hamaker dispersion forces) can then operate toward aggregation and precipitation. At higher salt concentrations, preferential hydration of salt ions can desolvate proteins, causing them to aggregate, precipitate, or crystallize (the salting-out effect). Molecular-thermodynamic models describing protein phase separation in concentrated aqueous salt solutions require physicochemical information about the interactions between protein molecules and salt ions. For example, models based on potential-of-mean-force descriptions of interactions in solution require information for ion–protein as well as protein–protein interactions.^{2–6}

This work explores the dependence of hen-egg-white lysozyme's net charge, z_p , and the interaction with chloride and potassium ions on solution pH and ionic strength using experimental results from hydrogen-ion titrations. Hydrogen-ion titrations have been conducted in potassium chloride solutions for lysozyme and 11 amino acids over a broad range of ionic strength and pH. From the ionic-strength dependence of the protein titration curves, ion-binding numbers have been calculated using a molecular-thermodynamic model derived by Fraaije and co-workers^{1,7,8} and are reported here. Discussion is presented on the effect of solution ionic strength on the surface

charge of lysozyme, on pK_a values of the various titratable groups, and on the protein titration curve.

2. Hydrogen-Ion Titrations of Proteins

In a protein molecule, hydrogen ions bind covalently to the side chains of acidic and basic amino acid residues and at the amino and carboxyl termini of the amino acid chain(s) of the protein. At any given pH, the protonation state of each titratable group depends on its hydrogen ion dissociation constant, or K_a . If the values of the individual K_a s of all the titratable groups are known, the net proton charge of the protein, z_p , may be calculated as a function of pH as follows. The hydrogen-ion dissociation equilibrium constant of site i , $K_{a,i}$, is given by

$$K_{a,i} = \frac{a_{H^+}a_{A_i}}{a_{HA_i}} \quad (1)$$

where a stands for activity. The hydrogen-ion activity is given by $a_{H^+} = c_{H^+}\gamma_{H^+}$, where c_{H^+} and γ_{H^+} are the molar concentration and the ionic-strength-dependent activity coefficient of the hydrogen ion, respectively. The activities of the protonated and deprotonated states are given by $a_{HA_i} = c_{HA_i}\gamma_{HA_i}$ and $a_{A_i} = c_{A_i}\gamma_{A_i}$, respectively. The logarithm of eq 1 yields

$$p^0H - p^0K_{a,i} = \log\left(\frac{c_{A_i}}{c_{HA_i}}\right) \quad (2)$$

where the concentration-based definitions $p^0H \equiv -\log c_{H^+}$ and $p^0K_{a,i} \equiv -\log(c_{H^+}c_{A_i}/c_{HA_i})$ are introduced. These are related to the conventional activity-based definitions $pH \equiv -\log a_{H^+}$ and $pK_{a,i} \equiv -\log K_{a,i}$ through the activity coefficients

$$p^0H = pH + \log \gamma_{H^+} \quad (3a)$$

$$p^0K_{a,i} = pK_{a,i} + \log(\gamma_{H^+}\gamma_{A_i}/\gamma_{HA_i}) \quad (3b)$$

From eqs 1 and 2, the net protein charge, z_p , is calculated as a function of pH. The net charge of the protein molecule also

* To whom correspondence should be addressed.

[†] University of California, Berkeley.

[‡] Present address: Bristol-Myers Squibb Pharmaceutical Research Institute, 1 Squibb Drive, New Brunswick, NJ 08903-0191. E-mail: kuehnerd@bms.com.

[§] Present address: Department of Chemical Engineering, University of Cambridge, Pembroke Street, Cambridge CB2 3RA, U.K. E-mail: je224@hermes.cam.ac.uk.

^{||} Present address: Department of Chemical Engineering, Technical University of Hamburg-Harburg, Eissendorfer Strasse 38, D-21071 Hamburg, Germany; email: fergg@tu-harburg.de.

[⊥] Lawrence Berkeley National Laboratory.

TABLE 1: pK_a Values for Titratable Groups in Hen-Egg-White Lysozyme from Various Authors and from Free Amino Acid Titrations

amino acid residue	exptl pK_a ref 17	calcd pK_a ref 12	calcd pK_a ref 14	amino acid titrations (0.1 M KCl)
N-term (Lys)	7.9	5.0	7.27	N-term: 9.21
Asp-18	2.0	2.6	3.00	Asp: 3.72
Asp-48	4.3	1.6	3.33	Glu: 4.17
Asp-52	3.4	8.5	5.66	His: 6.06
Asp-66	1.6	2.2	2.69	Tyr: 10.17
Asp-87	2.1	0.8	3.15	Lys: 10.81
Asp-101	4.5	4.3	3.37	Arg: 12.77
Asp-119	2.5	1.3	3.35	C-term: 2.32
Asp average	2.9	3.8	3.51	
Glu-7	2.6	1.2	2.60	
Glu-35	6.1	6.2	4.69	
His-15	5.8	2.4	6.71	
Lys-1	10.8	10.8	10.57	
Lys-13	10.5	10.1	10.75	
Lys-33	10.6	7.7	9.94	
Lys-96	10.8	8.9	9.82	
Lys-97	10.3	8.4	10.51	
Lys-116	10.4	9.7	10.22	
Lys average	10.6	9.3	10.30	
Tyr-20	10.3	12.1	12.00	
Tyr-23	9.8	10.1	10.89	
Tyr-53	12.1	18.8	16.89	
C-term (Leu)	3.1	2.2	3.10	

depends on the ionic strength of the solution. Addition of salt attenuates electrostatic interactions in the local microenvironment of each titratable group, altering the activity coefficients of the protonated and deprotonated states and thereby shifting the pK_a of that group. Since proteins are in essence large, conformationally complex polyelectrolytes, the experimental determination of the activity coefficients of individual titratable groups as a function of solution chemistry is difficult and has only recently become possible via NMR.^{9,10}

With the advent of powerful computational tools, many efforts have been made to calculate a priori the pK_a s of titratable side chains in hen-egg-white lysozyme and other well-studied proteins.^{11–16} In general, these methods describe the titration equilibrium for a given site as

$$pK_a = pK_{a,model} + \Delta pK_a \quad (4)$$

where $pK_{a,model}$ refers to a hypothetical case wherein the titrating group has no intramolecular electrostatic interactions with the rest of the protein. Approximate values of $pK_{a,model}$ may be obtained experimentally from titration of fully denatured proteins or end-blocked polypeptides containing the side chain of interest. The perturbation, ΔpK_a , contains all the electrostatic effects introduced by placing the titrating side chain in the environment of a native protein molecule. In an early computational study, Bashford and Karplus¹² calculated pK_a s for titratable groups in lysozyme at an ionic strength of 0.1 M, using crystallographic data to define lysozyme's shape and finite-difference methods to solve the linearized Poisson–Boltzmann equation for the electrostatic-potential profile around the molecule; pK_a s are shown in Table 1. This method assumes the protein structure to be rigid in its crystallographic shape. However, it has been recognized that the lack of conformational mobility of the side chains leads to overestimation of electrostatic pK_a perturbations. The physical rationale is as follows: when titration brings a residue into the charged state, the surrounding environment (solvent and protein) reorients in an effort to offset the charge, reducing the magnitude of the pK_a perturbation. Beroza and Case¹⁴ incorporated side chain flexibility, using conformational

sampling methods (see Table 1). Table 1 also lists “experimental” pK_a s regressed by Kuramitsu and Hamaguchi¹⁷ from lysozyme titration curves measured in 0.1 M potassium chloride solutions. The computed pK_a s of Beroza and Case show closer agreement, on average, with experimental results than those of Bashford and Karplus.

A conclusive example of the power of these models to describe the electrostatic environment around the protein is given by Glu-35 in lysozyme's active site. The experimentally observed value of the pK_a of Glu-35, 6.1, is abnormally high;^{9,17} for free glutamic acid, the side chain pK_a is 4.2. The deprotonated state of Glu-35 has a strong interaction with the negative charge of nearby Asp-52 and with the negative end of the macrodipole created by the α -helical conformation of residues 25–35.¹¹ These repulsive electrostatic interactions favor the protonated state of Glu-35, resulting in a large positive pK_a perturbation. Effects such as these cannot be described a priori with empirical models.

3. Titration Experiments

In a pH measurement, the measured electrode voltage, E , and the hydrogen ion activity, a_{H^+} , are related by a Nernst-type equation:

$$\begin{aligned} E &= E^{\text{ref}} + S \log a_{H^+} \\ &= E^{\text{ref}} - S[p^0H - \log \gamma_{H^+}] \end{aligned} \quad (5)$$

where E^{ref} is the electrode standard potential and S is the slope determined by an electrode-calibration titration prior to each protein titration. The hydrogen ion activity coefficient was calculated using Pitzer's model for multicomponent electrolyte solutions¹⁸; γ_{H^+} varied with ionic strength but was independent of hydrogen ion concentration over the range $2 < \text{pH} < 12$.

3.1. Electrode-Calibration Titration. Calibration titrations were performed by serial addition of aliquots of an alkaline titrant solution containing 0.1 M KOH to a potassium chloride solution (“blank”) previously acidified with HCl to approximately pH 2.5. The blank and the titrant solutions had the same total ionic strength. Aliquots of the alkaline titrant solution were added until the solution pH reached approximately 11.5, yielding data in the form $\{E, V^{\text{added}}\}$. Mass balances for hydrogen and hydroxide ions enabled calculation of p^0H (via the water dissociation reaction) and the electrode slope and intercept. Values of E^{ref} and S obtained for each electrode calibration were considered valid for 1 day at most. Separate calibration titrations were performed for each protein or amino acid titration, which were carried out immediately following the calibration titrations.

3.2. Protein and Amino Acid Titrations. For titration solutions containing protein or amino acid, a modified set of mass balances accounted for the reaction of hydrogen ion with the protein or amino acid. With these mass balances and the electrode slope and intercept obtained from the calibration titration, the change in the charge of the protein or amino acid with p^0H was calculated. All titration curves reported here are referenced to the isoelectric point (where $z_p = 0$) of lysozyme, $p^0I = 11.16$. The concentration-based isoelectric point, p^0I , is given by $p^0I = pI + \log \gamma_{H^+}$ and was assumed not to vary with ionic strength, as discussed below.

3.3. Materials. Hen-egg-white lysozyme ($M = 14\,500$ g/mol) was obtained from Sigma Chemical Company, St. Louis, MO (L-2879; CAS no. 9066-59-5; grade VI, chloride, $3\times$ crystallized). The following L-amino acids were obtained from Sigma and were used without further purification: alanine (A-5824;

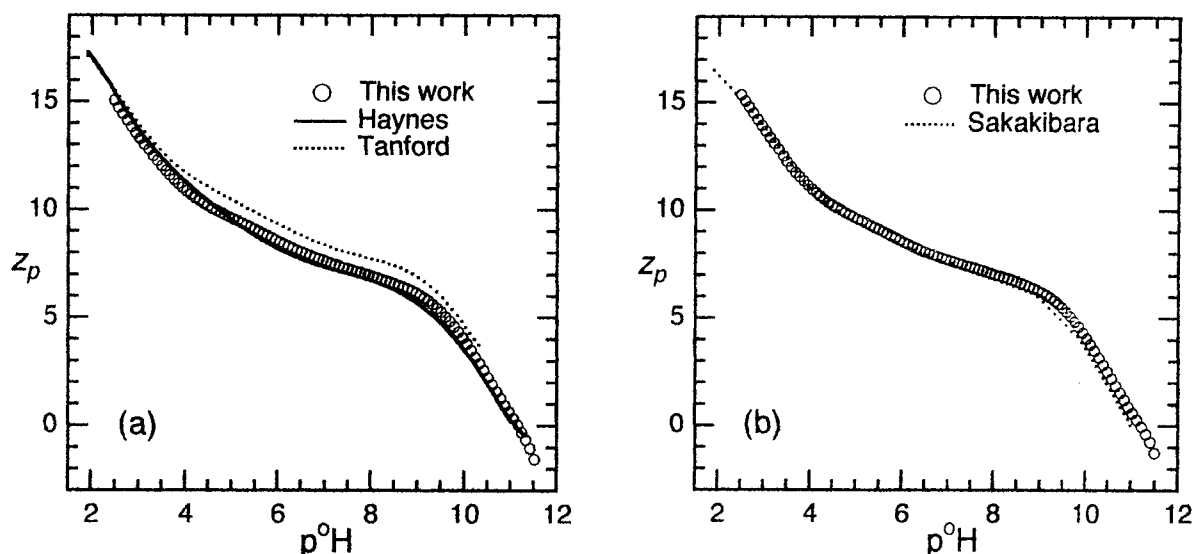


Figure 1. Experimental hydrogen ion titration curves for hen-egg-white lysozyme in solutions of potassium chloride at ionic strengths (a) 0.1 M and (b) 0.2 M.

CAS no. 56-41-7), arginine (A-5006; CAS no. 74-79-3; free base), asparagine (A-8824; CAS no. 5794-13-8; monohydrate), aspartic acid (A-8949; CAS no. 56-84-8; free acid), cysteine (C-7755; CAS no. 52-90-4; free base), glutamic acid (G-6904; CAS no. 56-86-0; free acid), histidine (H-8776; CAS no. 71-00-1; free base), isoleucine (I-7268; CAS no. 73-32-5), leucine (L-5652; CAS no. 61-90-5), lysine (L-5501; CAS no. 56-87-1; free base), and tyrosine (T-8909; CAS no. 60-18-4; free base). Potassium hydrogen phthalate (CAS no. 877-24-7) was obtained from Aldrich Chemical Co., oven-dried, and stored under vacuum. Standardized stock solutions of hydrochloric acid (CAS no. 7647-01-0) and potassium hydroxide (CAS no. 1310-58-3) of concentrations 0.995–1.005 N were purchased from Fisher Scientific, along with crystalline potassium chloride (CAS no. 7447-40-7; ACS grade). Distilled, deionized, and degassed water was used to make all solutions.

Protein solutions were prepared by dissolving lysozyme powder in water to approximately 80 mg/mL and acidifying to pH 3 with hydrochloric acid stock solution. Gel-permeation chromatography was used to remove the ovalbumin and conalbumin contaminants from Sigma L-2879 lysozyme.^{19,20} Lysozyme-rich eluate was concentrated to approximately 10 g/L via ultrafiltration through Diaflo YM10 membranes (Amicon; 10 000 g/mol MWCO) and dialyzed in Spectrapor membrane tubing (Spectrum; 6–8000 g/mol MWCO) against 50 volumes of potassium chloride solution of the desired ionic strength. Lysozyme concentration was determined by ultraviolet spectrophotometry using an extinction coefficient of $\epsilon_{280\text{nm}}^{25^\circ\text{C}} = 2.635 \text{ L/(g cm)}$.²¹ Lysozyme concentration varied between 7 and 12 g/L (0.5–0.8 mmol/L); no effect of protein concentration on titration results was observed within this concentration range. Amino-acid solutions were prepared by dissolving in water the dry amino-acid powder and sufficient crystalline potassium chloride to prepare a solution of the desired ionic strength. Amino-acid concentrations were never greater than 5 mmol/L.

The exact concentrations of H^+ and OH^- in the acidic and alkaline titrant solutions were determined by first titrating the alkaline titrant against a standard solution containing a known amount of potassium hydrogen phthalate, then titrating the acidic titrant against a specified amount of the alkaline titrant. These titrant-concentration assays were performed at least in triplicate. A solution of 0.15% (v/v) phenolphthalein in ethanol was used as indicator.

3.4. Automated Titration Apparatus. Titration experiments were conducted in an airtight 100 mL, jacketed glass vessel sealed by a Plexiglas lid with ports for titrant injection lines, gas lines, and the pH electrode. Vessel temperature was maintained at 25 °C (± 0.1 °C) by recirculation of water through the vessel jacket and a thermostated bath. The headspace was swept with argon at very small positive pressure during the titrations to remove airborne carbon dioxide. Argon was passed through a column packed with Drierite and acid-gas-specific molecular sieves to remove trace water and carbon dioxide and then was resaturated by sparging through a gas-washing bottle filled with degassed, distilled, deionized water. Titrant aliquots of specified volume were injected through a fritted line by a Dosimat 665 precision pump (Metrohm; Westbury, NY). Solutions in the titration vessel were agitated gently by a magnetic stirrer to speed pH equilibration after injection of each titrant aliquot. Hydrogen ion activity was measured using a Ross combination semimicroelectrode (Orion; Boston, MA), and the electrode response, E , was recorded by a control PC via an analog-to-digital converter board (Keithley Metrabyte DAS-1400; Cleveland, OH). Control software allowed automation of all experiments; titrant aliquots were injected until the pH end point was reached, with sufficient time for electrode equilibration between aliquot injections. Data in the form $\{E, V_{\text{added}}\}$ were saved for subsequent analysis. At any p^0H value between 2.5 and 11.5, reproducibility between replicate titration curves was usually within 0.1 valence units; this variation was taken as the intrinsic uncertainty of the experimental method.

4. Results

4.1. Experimental and Theoretical Protein Titration Curves. Figure 1 compares the titration curve for lysozyme in potassium chloride solutions with other experimental results in the literature. The titration curve of Haynes et al.,²² shown in Figure 1a, agrees with our measurements to within an average charge deviation of 0.3 units over the entire p^0H range, with a maximum deviation of 0.8 charge units at $\text{p}^0\text{H} \approx 9.3$. The older data of Tanford and Roxby²³ deviate significantly; these deviations may reflect the presence of protein impurities in their titrations. Similar agreement is shown in Figure 1b for the titration data reported here for solutions containing 0.2 M potassium chloride and the data of Sakakibara and Hamaguchi.²⁴

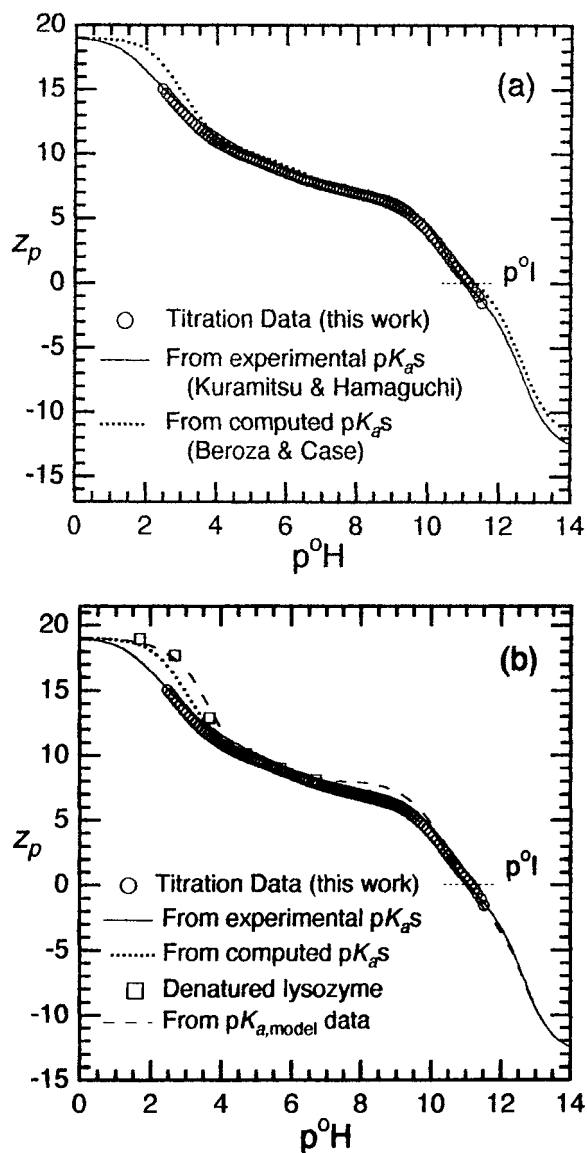


Figure 2. Experimental and theoretical titration curves for hen-egg-white lysozyme in 0.1 M potassium chloride solutions.

Figure 2a shows the experimental titration curve for hen-egg-white lysozyme measured in this work for solutions containing 0.1 M potassium chloride. Also shown in Figure 2a are two other titration curves for lysozyme calculated from the experimental pK_a s of Kuramitsu and Hamaguchi (solid line) and Beroza and Case (dotted line) listed in Table 1. Here, p^0K_a s were obtained from eq 3b, with γ_{H^+} calculated from Pitzer's model.¹⁸ In these experiments lysozyme was dilute, and the assumption $\gamma_{HA_i} = \gamma_{A_i} = 1$ was made. There are two p^0H regions in Figure 2a where the theoretical titration curve calculated from the pK_a s computed by Beroza and Case differs sufficiently from our experimental curve (and from the curve calculated from the pK_a s of Kuramitsu and Hamaguchi) to warrant discussion: the acidic region where $p^0H < 4$ and the alkaline region where $p^0H > 11$. For $p^0H < 4$, the titrating groups are the side chains of the seven aspartic acid residues and Glu-7, and the C-terminal carboxyl group. A reasonable way to compare the differences between titration curves in this p^0H region is to compare the average value of the aspartic-acid side chain pK_a . Table 1 shows that the average value of the aspartic acid side chain pK_a is 2.9 for the results of Kuramitsu and Hamaguchi and 3.51 for the results of Beroza and Case. At a given p^0H , titratable groups

with higher pK_a s remain more positively charged than groups with lower pK_a s. Similarly, for $p^0H > 11$, the theoretical titration curve of Beroza and Case is shifted by up to +1 charge unit relative to the curve calculated from the experimental pK_a s of Kuramitsu and Hamaguchi because the theoretical side chain pK_a s of Tyr-20 and Tyr-23 are 1–2 pH units higher than the experimental values. Furthermore, in the limit of highest p^0H , all titration curves should converge to $z_p = -13$. However, Beroza and Case assert that the pK_a is 16.89 for Tyr-53, an unrealistically high value, explaining why their titration curve remains offset by +1 charge unit from the two experimental titration curves as p^0H increases to 14. If not for the unusually high pK_a s computed for all three of the lysozyme's tyrosyl side chains, the theoretical titration curve would be in excellent agreement with the experimental titration curves for p^0H greater than 4.

As discussed above, any ΔpK_a is relative to some $pK_{a,model}$ that, in theory, reflects no electrostatic interactions external to the titrating site itself. To obtain a simple experimental estimate of $pK_{a,model}$ for the titratable groups in lysozyme, free amino acid titrations were conducted in potassium chloride solutions for each of the amino acids bearing titratable groups found in lysozyme. Results from solutions with an ionic strength of 0.1 M are shown in Table 1; complete results for ionic strengths to 3.0 M are given in Table 2. The side chain pK_a s measured in these titrations are not entirely free of the effect of intramolecular electrostatic interactions because for amino acid monomers, the amino- and carboxy-terminal titratable groups are in relatively close molecular proximity to the side chain titratable groups. More accurate estimates of the $pK_{a,model}$ values would in principle be obtained by titration of denatured proteins or end-blocked polypeptides. However, for the purpose of demonstrating the presence of pK_a perturbations in lysozyme, titration of monopeptides was considered sufficient.

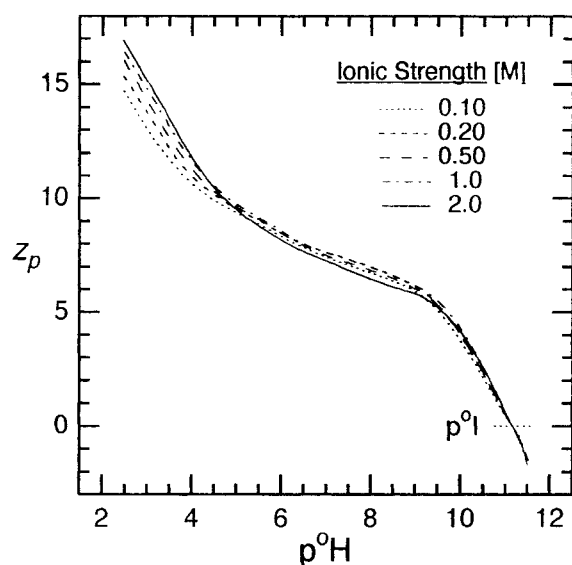
Figure 2b shows all titration curves in Figure 2a, with the addition of two new curves: one (dashed line) calculated from the $pK_{a,model}$ values measured from the free amino-acid titrations conducted in 0.1 M potassium chloride solutions; and one showing titration data (open squares) for denatured lysozyme in 6 M guanidine–hydrochloride solution for p^0H less than 7.²³ Good agreement of these two additional curves validates the choice of amino acid monomers as model compounds for the acidic p^0H region. The aspartic acid side chain $pK_{a,model}$ measured in free aspartic acid solution is 3.72, 0.8 pH unit higher than the average experimental pK_a of Kuramitsu and Hamaguchi. Consequently, because there are seven aspartic acid residues in lysozyme, the titration curve calculated from the free amino acid $pK_{a,model}$ values (dashed line) shows a significantly higher net protein charge than either of the experimental lysozyme titration curves for $p^0H < 4$. The theoretical titration curve calculated from the pK_a s of Beroza and Case (shown in Figure 2b for $p^0H < 4$ only) lies between the titration curve calculated from the free amino-acid $pK_{a,model}$ s and the experimental curves, indicating that the electrostatic modeling efforts of Beroza and Case were partially successful in quantifying aspartic acid side chain ΔpK_a s in lysozyme.

None of these authors investigated the hydrogen-ion equilibria of the 11 arginine side chains in lysozyme. The pK_a s of these groups are expected to be quite alkaline; the pK_a for the arginine side chain in the free amino acid titrations reported here is 12.77 in solutions with 0.1 M potassium chloride concentration, well above the p^0H range used in most titration experiments with lysozyme. In computing the pK_a s of other titratable groups in

TABLE 2: Amino Acid Carboxy-Terminal, Amino-Terminal, and Side Chain pK_a s Measured in Solutions of Potassium Chloride with Ionic Strengths 0.1, 1.0, and 3.0 M at 25 °C ^a

amino acid	<i>I</i> = 0.1 M			<i>I</i> = 1.0 M			<i>I</i> = 3.0 M		
	C-term pK_a	N-term pK_a	side-chain pK_a	C-term pK_a	N-term pK_a	side-chain pK_a	C-term pK_a	N-term pK_a	side-chain pK_a
alanine	2.36	9.86		2.44	9.76		2.72	10.10	
arginine	2.08	9.09	12.77	2.27	9.28	12.87	2.55	9.63	12.83
asparagine	2.18	8.73		2.28	8.83		2.46	9.13	
aspartic acid	2.00	9.72	3.72	2.05	9.58	3.68	2.26	9.89	3.94
cysteine	1.95	10.36	8.23	2.01	10.26	8.24	2.27	10.39	8.44
glutamic acid	2.22	9.64	4.17	2.18	9.49	4.11	2.50	9.74	4.43
histidine	1.71	9.15	6.06	1.94	9.18	6.26	2.15	9.45	6.60
isoleucine	2.33	9.64		2.43	9.72		2.71	10.04	
leucine	2.32	9.64		2.43	9.75		2.70	10.01	
lysine	2.10	9.21	10.81	2.29	9.39	10.85	2.62	9.70	11.01
tyrosine	2.22	9.04	10.17	2.33	9.09	10.02	2.62	9.36	10.18

^a Arginyl side chain pK_a s were obtained by extrapolation of the titration curve past the upper p^0H end point (usually approximately 12.5).

**Figure 3.** Dependence of experimental titration curves on solution ionic strength for hen-egg-white lysozyme in potassium chloride solutions.

the protein, Beroza and Case assumed that the arginine side chains are always protonated. Furthermore, the pK_a regression technique of Kuramitsu and Hamaguchi was not sufficiently sensitive to extract 11 unique pK_a s from such a narrow region of extreme p^0H . It is reasonable to assume that the pK_a s of these groups in the protein are perturbed, but the magnitudes of the perturbations have not yet been quantified. Therefore, in calculating the titration curves shown in Figure 2, the free amino-acid value of arginine's side chain pK_a was used as an approximation, in effect introducing 11 identical titratable groups with $pK_a = 12.77$.

Figure 3 shows experimental hydrogen-ion titration curves measured for lysozyme at 25 °C in solutions where the potassium chloride ionic strength varied from 0.1 to 2.0 M. Each curve represents an average of between two and seven titration experiments. At $p^0H = 2.5$, the curves are well separated and show a trend of increasing net protein charge with increasing solution ionic strength. As p^0H rises, the curves converge; for $p^0H > 5$, the titration curves for ionic strengths to 1.0 M all show net protein charges that agree to within 0.5 charge units. The titration curve for 2.0 M ionic strength differs; at $p^0H = 4.3$, it crosses the 1.0 M curve and shows the lowest net protein charge of any titration curve for p^0H between 5.2 and 9.1. Experimentally, the 2.0 M titration solutions were not as stable as those with lower ionic strengths; for p^0H greater than 9,

protein macroaggregates were often observed in the titration vessel, and pH-electrode equilibration after each aliquot addition was less reliable. Hence, the 2.0 M data may not truly reflect the solution behavior of fully solvated, nonaggregated lysozyme molecules, even in the acidic branch of the titration curve. Although lysozyme is known to possess a monomer–dimer equilibrium at p^0H above 5 in low ionic-strength solutions,²¹ it was assumed not to affect the titration behavior of the protein.

All titration curves in Figure 3 are referenced to a common isoelectric point, $p^0I = 11.16$, assumed constant with respect to ionic strength. The p^0I would exhibit an ionic-strength dependence if the hydrogen ion equilibria of titratable groups having pK_a s near the p^0I were dependent on ionic strength. In lysozyme, these groups are the six lysine residues. Table 2 shows that the $pK_{a,model}$ value for lysine is 10.8 for ionic strengths 0.1 and 1.0 M. Further, the average lysine pK_a s in Table 1, both those regressed by Kuramitsu and Hamaguchi and those calculated by Beroza and Case, agree with $pK_{a,model}$ to within 0.5 p^0H units at 0.1 M ionic strength. Hence, the isoelectric point of lysozyme is not assumed to depend on ionic strength.

4.2. Lysozyme Surface-Charge Interactions. Rasmol molecular-graphics visualization of hen-egg-white lysozyme (Brookhaven PDB structure 2LYZ) shows that most titratable groups reside on or near the molecular surface. Therefore, in the extreme acidic limit, the surface of the lysozyme is highly positively charged. As the p^0H increases, the low- pK_a groups (i.e., the aspartic-acid and glutamic-acid side chains) deprotonate and become negatively charged, interacting favorably with the positively charged lysine and arginine residues. The presence of the positively charged lysine and arginine groups on the surface favors deprotonation of the acidic residues, reflected as negative pK_a perturbations for these residues. Table 1 shows that the experimental ΔpK_a is, on average, -0.8 pH units for the aspartic acid residues and -1.6 pH units for Glu-7, relative to the $pK_{a,model}$ values measured for free amino acids in 0.1 M potassium chloride solution. (The positive pK_a perturbation of Glu-35 has been explained above.) These negative ΔpK_a perturbations produce the downward shift in the experimental titration curve, relative to the curve calculated from the $pK_{a,model}$ values, observed in Figure 2b.

As the ionic strength increases, electrostatic interactions between solvent-accessible surface residues diminish because of dielectric screening. Therefore, addition of mobile salt ions to the protein solution reduces the magnitude of the negative pK_a perturbations of the acidic groups, giving pK_a s that increase with rising ionic strength, as verified experimentally by Abe et al.¹⁰ These authors used two-dimensional NMR methods to

probe the effect of ionic strength on the hydrogen ion equilibria of the acidic residues of hen-egg-white and turkey-egg-white lysozymes, over a range of salt concentrations from 5 to 400 mM, in sodium chloride solutions. Hence, for the acidic residues, as the ionic strength increases, dielectric screening of surface electrostatic interactions also increases, negative pK_a s perturbations relax, and the titration curves shift upward to show a higher net protein charge at any given p^0H , as shown in Figure 3. Similarly, for any p^0H above the isoelectric point, the protein has a net negative charge and pK_a perturbations increase the protein's net charge. In general, these are positive pK_a perturbations for the alkaline titratable groups. As the ionic strength increases at high p^0H , screening of surface electrostatic interactions decreases the positive pK_a perturbations and the titration curve shifts downward. On a plot such as Figure 3, these ionic-strength-dependent pK_a shifts produce a clockwise rotation of the titration curve around the isoelectric point as ionic strength increases. This rotation phenomenon has been previously reported for other soluble globular proteins where most of the titratable residues are surface-accessible.^{25,26} However, it is not readily observed in Figure 3 because the lysozyme's isoelectric point is so high.

4.3. Ion Binding to Lysozyme. Lysozyme is known to bind chloride ions in a manner that depends on both the solution pH and the ionic strength.²⁷ To construct comprehensive molecular descriptions of protein-salt interactions in aqueous salt solutions, especially at ionic strengths where salt-induced phase equilibria occur, it is necessary to have experimental information about the extent of ion binding by protein. Fraaije and Lyklema^{1,7,8} have developed a general molecular-thermodynamic description of ion binding that requires knowledge of the ionic-strength dependence of hydrogen ion titration curves. These authors have applied this model to predict binding of chloride ions to bovine serum albumin.¹ The central principle of this theory is that the binding number, r_i , of any dissolved species i is related to the binding numbers of all other species. Hence, hydrogen ion binding information contained in protein titration data is required to obtain (in our case) potassium ion and chloride ion binding numbers. The binding number for chloride ion, for example, depends on both ionic strength and p^0H and is expressed in terms of the protein charge by

$$r_{Cl^-} = \frac{z_p}{2} - \frac{1}{2} \int_{pI}^{p^0H} \delta_{a/b} d(p^0H) \quad (6)$$

where the Esin-Markov coefficient $\delta_{a/b}$ is defined as

$$\delta_{a/b} \equiv \left(\frac{\partial z_p}{\partial \log a_s} \right)_{p^0H, c_p} \quad (7)$$

and incorporates the ionic-strength dependence of the protein titration data. The salt activity is $a_s = m\gamma^\pm$, where m is the salt molality and γ^\pm is the mean ionic activity coefficient, obtained here from Pitzer's model.¹⁸ The potassium binding number is calculated from the overall electroneutrality relation for the protein molecule plus its surrounding dielectric double layer:

$$r_{K^+} = r_{Cl^-} - z_p \quad (8)$$

In the context of this general model, ion "binding" refers to the preferential interaction of ions with the protein, relative to the bulk solution, either by binding tightly to the protein or by associating loosely in the diffuse double layer.

The protein net charge, z_p , was obtained as a function of p^0H and ionic strength from the lysozyme titration curves of Figure

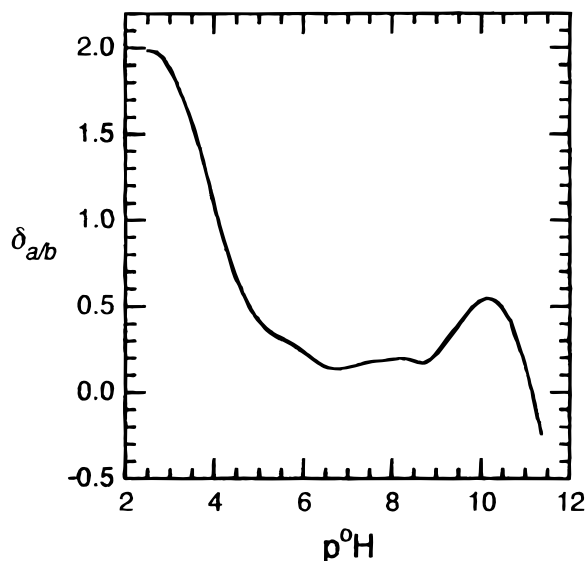


Figure 4. Dependence of Esin-Markov coefficient on p^0H for hen-egg-white lysozyme in 0.1 M potassium chloride solutions.

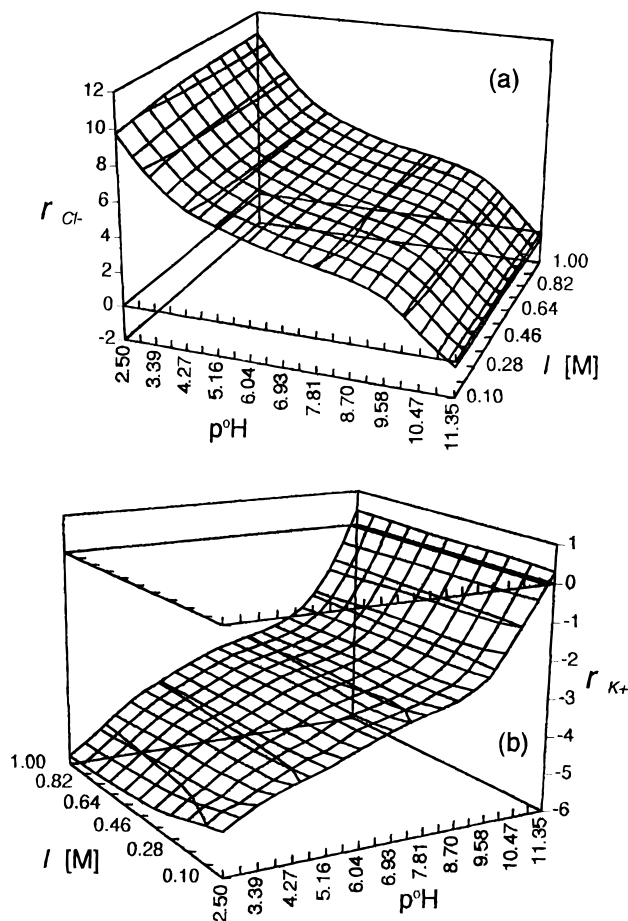


Figure 5. (a) Chloride-ion binding numbers in solutions of hen-egg-white lysozyme and potassium chloride. (b) Potassium ion binding numbers in solutions of hen-egg-white lysozyme and potassium chloride.

3. Multivariable regression was used to fit the titration data to the p^0H and ionic-strength axes simultaneously. Calculations were implemented using MathCad Professional 7.0 software. Coefficients $\delta_{a/b}$ were obtained by establishing a fit of z_p to $\log a_s$ at each p^0H , for ionic strengths to 1.0 M. The 2.0 M titration curve was not included in the $\delta_{a/b}$ calculations because it behaves in a manner inconsistent with the trend of the lower-

ionic-strength curves, as discussed above. Coefficient $\delta_{a/b}$ is shown in Figure 4 as a function of p^0H for an ionic strength of 0.1 M. The lysozyme titration curves show the greatest ionic-strength dependence for p^0H less than 5; consequently, this p^0H region is where the values of $\delta_{a/b}$ are largest. For $p^0I < p^0H < 11.35$ (the upper p^0H limit in these calculations), $\delta_{a/b}$ in Figure 4 has a small negative value as a result of the inversion of the ionic-strength dependence of the lysozyme titration curves at p^0H above the isoelectric point.

Parts a and b of Figure 5 show, respectively, binding numbers for chloride ions and potassium ions to lysozyme, calculated from eqs 6–8. These numbers reflect the preferential interaction of the ions with lysozyme, relative to their concentrations in the reference solution (the lysozyme-free salt solution). Chloride binding is highest at low p^0H , where the protein is most positively charged and counterions partition preferentially into the diffuse double layer. At p^0H above the isoelectric point, where the lysozyme bears a negative net charge, a slight “negative” binding occurs. This corresponds to expulsion of a chloride anion, now a co-ion, from the double layer. The ionic strength dependence of chloride binding is greatest at low p^0H where the protein is highly charged. As ionic strength rises, the net charge of the protein increases, as shown in Figure 3; consequently, more counterions selectively partition into the diffuse double layer. As the p^0H increases toward the isoelectric point, the dependence of the protein net charge on ionic strength decreases, as previously discussed, and therefore, the ion-binding numbers also depend less on ionic strength. Figure 5b shows that potassium ion binding exhibits trends with p^0H and ionic strength opposite to those of the chloride ion, as determined by the requirement of overall electroneutrality of the protein molecule plus double layer.

5. Conclusion

Hydrogen-ion titrations of hen-egg-white lysozyme were conducted over the p^0H range 2.5–11.5, with ionic strengths to 2.0 M. These data provided two kinds of information useful for a molecular-thermodynamic description of protein–solution behavior. First, the function z_p allows direct evaluation of net protein charge over a wide range of solution pH and ionic strength. An independent measure of the protein net charge reduces the experimental effort in the regression of other adjustable parameters in any model for describing thermodynamic properties of protein solutions. Second, binding numbers for chloride and potassium ions were obtained from the ionic-strength dependence of the hydrogen-ion titration curves. As modern trends in molecular-thermodynamic models move toward incorporating salt ions as discrete species in solution, physicochemical data will be required to quantify interactions between salt ions and proteins; ion-binding numbers provide such information. For example, the multicomponent adhesive-hard-sphere model, used previously to describe ion clustering,^{5,28} relates binding numbers to intermolecular potential parameters. Also, titrations were conducted for 11 of the 20 natural L-amino acids in potassium chloride solutions at ionic strengths to 3.0 M. Measured pK_a s of N-terminal, C-terminal, and side-chain hydrogen-ion equilibria are reported. Because we have not found any amino acid pK_a s in the literature for ionic strengths greater

than 1.0 M, the data given here provide significant additions to the existing base of knowledge of amino-acid hydrogen-ion equilibria in electrolyte solutions.

Glossary

a_i	activity of species i
c_i	molar concentration of species i
E	electrode voltage response
E^{ref}	electrode reference potential
I	ionic strength
$K_{a,i}$	hydrogen ion dissociation equilibrium constant of titratable group i
m_i	molal concentration of species i
r_i	binding number of species i
S	electrode slope
z_p, z_i	net charge of protein, net charge of species i
γ_i	single ion activity coefficient of ionic species i
γ^\pm	mean ionic activity coefficient
$\delta_{a/b}$	Esin–Markov coefficient

References and Notes

- (1) Fraaije, J. G. E. M.; Lyklema, J. *Biophys. Chem.* **1991**, *39*, 31–44.
- (2) Kuehner, D. E.; Blanch, H. W.; Prausnitz, J. M. *Fluid Phase Equilib.* **1996**, *116*, 140–147.
- (3) Kuehner, D. E.; Heyer, C.; Rämisch, C.; Fornefeld, U. M.; Blanch, H. W.; Prausnitz, J. M. *Biophys. J.* **1997**, *73*, 3211–3224.
- (4) Vlachy, V.; Blanch, H. W.; Prausnitz, J. M. *AIChE J.* **1993**, *39*, 215–223.
- (5) Chiew, Y. C.; Kuehner, D. E.; Blanch, H. W.; Prausnitz, J. M. *AIChE J.* **1995**, *41*, 2150–2159.
- (6) Coen, C. J.; Blanch, H. W.; Prausnitz, J. M. *AIChE J.* **1995**, *41*, 996–1004.
- (7) Fraaije, J. G. E. M.; Murriss, R. M.; Norde, W.; Lyklema, J. *Biophys. Chem.* **1991**, *40*, 303–315.
- (8) Fraaije, J. G. E. M.; Norde, W.; Lyklema, J. *Biophys. Chem.* **1991**, *40*, 317–327.
- (9) Bartik, K.; Redfield, C.; Dobson, C. M. *Biophys. J.* **1994**, *66*, 1180–1184.
- (10) Abe, Y.; Ueda, T.; Iwashita, H.; Hashimoto, Y.; Motoshima, H.; Tanaka, Y.; Imoto, T. *J. Biochem.* **1995**, *118*, 946–952.
- (11) Spassov, V.; Karshikov, A.; Atanasov, B. *Biochim. Biophys. Acta* **1989**, *999*, 1–6.
- (12) Bashford, D.; Karplus, M. *Biochemistry* **1990**, *29*, 10219–10225.
- (13) Bashford, D.; Karplus, M. *J. Phys. Chem.* **1991**, *95*, 9556–9561.
- (14) Beroza, P.; Case, D. A. *J. Phys. Chem.* **1996**, *100*, 20156–20163.
- (15) You, T. J.; Bashford, D. *Biophys. J.* **1995**, *69*, 1721–1733.
- (16) Gibas, C.; Subramaniam, S. *Biophys. J.* **1996**, *71*, 138–147.
- (17) Kuramitsu, S.; Hamaguchi, K. *J. Biochem.* **1980**, *87*, 1215–1219.
- (18) Pitzer, K. S. *Activity Coefficients in Electrolyte Solutions*, 2nd ed.; CRC Press: Boca Raton, FL, 1991.
- (19) Lorber, B.; Skouri, M.; Munch, J.-P.; Giegé, R. *J. Cryst. Growth* **1993**, *128*, 1203–1211.
- (20) Skouri, M.; Lorber, B.; Giegé, R.; Munch, J.-P.; Candau, J. S. *J. Cryst. Growth* **1995**, *152*, 209–220.
- (21) Sophianopoulos, A. J.; Van Holde, K. E. *J. Biol. Chem.* **1964**, *239*, 2516–2524.
- (22) Haynes, C. A.; Sliwinsky, E.; Norde, W. *J. Colloid Interface Sci.* **1994**, *164*, 394–409.
- (23) Tanford, C.; Roxby, R. *Biochemistry* **1972**, *11*, 2192–2198.
- (24) Sakakibara, R.; Hamaguchi, K. *J. Biochem.* **1968**, *64*, 613–618.
- (25) Luo, C. Protein Charge and Ion Binding in High Ionic Strength Electrolyte Solutions. M.S. Thesis, University of California, Berkeley, 1997.
- (26) Edsall, J. T. Proteins as Acids and Bases. In *Proteins, Amino Acids, and Peptides*; Cohn, E. J., Edsall, J. T., Eds.; Reinhold: New York, 1943.
- (27) Carr, C. *Arch. Biochem. Biophys.* **1953**, *46*, 417–423.
- (28) Barboy, B.; Tenne, R. *Chem. Phys.* **1979**, *38*, 369.